RSC Advances

ROYAL SOCIETY OF CHEMISTRY

www.rsc.org/advances

Journal Name

ARTICLE

Sol-Gel-Processed (001)-Textured $BiFeO_3$ Thin Films on Pt(111)/Ti/SiO_2/Si Substrates with PbO Seeding Nanocrystals

Received 00th January 20xx,
Accepted 00th January 20xx

DOI: 10.1039/x0xx00000x

www.rsc.org/

Wei Sun, Zhen Zhou and Jing-Feng Li*

50 to 200-nm-thick $BiFeO_3$ thin films were fabricated on Pt(111)/Ti/SiO_2/Si substrates using the sol–gel method. A PbO seeding layer was introduced between $BiFeO_3$ films and the platinum electrode surface, which was found to be effective for the formation of (001)-textured $BiFeO_3$ structure. A high degree of (001) orientation up to 98.3% was achieved in a 200-nm-thick film via a layer-by-layer annealing process. Cross-section images by scanning electron microscopy revealed a columnar crystal structure, which was consistent with the high texturing degree enhanced by layer-by-layer annealing method. By investigating dielectric, ferroelectric and piezoelectric properties of the randomly oriented and (001)-oriented films, it was revealed that significant enhancements of dielectric and piezoelectric properties were achieved in textured samples. The texturing mechanism was also discussed.

1 Introduction

Ferroelectric and piezoelectric thin films have always been a research hotspot for applications in nonvolatile ferroelectric random access memories (FeRAM), microelectromechanical system (MEMS) and high frequency electrical components.[1-3] $BiFeO_3$ is the only room-temperature multiferroic material with high Curie temperature (T_c ~ 870 °C) and large remanent polarization (P_r ~ 100 μC cm^{-2}), which has been drawing intensive attention also as a promising candidate for ferroelectric and piezoelectric applications.[4-6] $BiFeO_3$ possesses a *R3c* distorted perovskite structure and can be denoted as a pseudocubic structure with lattice parameter a=3.96 Å and α=89.6°.[7,8] $[111]_{pc}$ is the spontaneous polarization direction of $BiFeO_3$ along which P_r reaches highest,[4,5] while $(001)_{pc}$ epitaxial $BiFeO_3$ film exhibits the best polarization fatigue behaviour among different orientations, which may result from the flexibility of 71° domain switching,[9] indicating the anisotropic properties of $BiFeO_3$. Hence, it is important to control the crystallographic orientation of $BiFeO_3$ thin films depending on the applications. Although it is possible to fabricate epitaxial $BiFeO_3$ films by pulse laser deposition (PLD) method, the process is complicated and needs single crystal substrates and special deposition equipment.[4,6,10] It is therefore still highly desired to obtain $BiFeO_3$ films with a certain orientation using a simple sol-gel process on the conventional silicon wafers, which are widely in modern electronic industry.[11-13] Certainly, some studies have been done about the sol-gel processing of textured $BiFeO_3$ thin films.[14] For example, Chang *et al.* reported (001)-oriented $BiFeO_3$ on a glass substrate by reducing the thickness of Pt electrode *via* sol-gel method.[15] Kariya *et al.* reported (100)-orientated $BiFeO_3$ thin films by introducing a $LaNiO_3$ buffer layer.[16] Nevertheless, it is clear the researches on sol-gel-processed textured $BiFeO_3$ films on silicon wafers are very limited. In particular, more studies on textured $BiFeO_3$ films with sufficiently thickness for piezoelectric applications are needed.

This work was conducted under the motivation to fabricate highly (001)-textured $BiFeO_3$ films on Pt(111)/Ti/SiO_2/Si substrates by the sol-gel method, which is suitable for large-scale film fabrication. PbO seeds were used because our previous works have proved that PbO seeding layer could induce (001)-textured perovskite Pb(Zr, Ti)O_3 (PZT) films on silicon wafers.[17,18] Such a seeding process was found also effective for $BiScO_3$-$PbTiO_3$.[19-21]

To search for the optimal texturing process, layer-by-layer and one-step annealing methods were used separately and a series of films with varied thicknesses were prepared to clarify the annealing process effect on texturing. Highly (001)-oriented structure with columnar crystal feature was obtained in 200-nm-thick films prepared by the layer-by-layer annealing procedure. The electrical properties were characterized and compared with the non-textured thin films, and enhancements on dielectric, ferroelectric and piezoelectric performances were found in the textured $BiFeO_3$ thin films. The relationship among orientation degree and thickness as well as the annealing procedures was also discussed.

2 Experimental

Synthesis

State Key Laboratory of New Ceramics and Fine Processing, School of Materials Science and Engineering, Tsinghua University, 100084 Beijing, P. R. China. E-mail: jingfeng@mail.tsinghua.edu.cn

Trihydrated lead acetate [$Pb(CH_3COO)_2 \cdot 3H_2O$] was dissolved into 2-methoxyethanol (2-MOE). An appropriate amount of formamide and acetylacetone were added for stabilization. The concentration of PbO solution was diluted to 0.02 mol L^{-1}. After the solution being refluxed for 4 h at 128 °C to remove H_2O, PbO gel was obtained. The PbO precursor was deposited onto the Pt(111)/Ti/SiO_2/Si substrates by spin coating at 4000 rpm and then annealed at 500 °C for 120 s in a rapid thermal process furnace. Bismuth nitrate [$Bi(NO_3)_3 \cdot 5H_2O$] and iron nitrate [$Fe(NO_3)_3 \cdot 9H_2O$] were used as the starting materials and 2-MOE as the solvent to achieve the solution for preparing $BiFeO_3$. To compensate for the loss during heat treatment, 7% excessive Bi was added. Citric acid was added into the solution as the chelating agent. After stirring for 4 h and aging for 48 h, $BiFeO_3$ precursor was prepared and the concentration was 0.25 mol L^{-1}. Then, the precursor solution was spin-coated on platinized silicon substrates with PbO seeds onside. Afterwards, two different crystallization routes were adopted. One is layer-by-layer annealing, which means that after the spin coating, the sample was dried at 100 °C, pyrolyzed at 400 °C and annealed at 550 °C and this coating-drying-pyrolysis-annealing process was repeated several times to reach the desired thickness. The other is one-step annealing, which means that each layer was dried, pyrolyzed and then the coating-drying-pyrolysis process was repeated, and finally the sample with the predetermined thickness was annealed for one time. Samples prepared by two methods were denoted as PbO+LBL and PbO+OS for abbreviation, respectively. For comparison, $BiFeO_3$ was also deposited directly on Pt(111)/Ti/SiO_2/Si substrates without PbO seeds following these two paths, denoted as LBL and OS, respectively. For all four kinds of samples prepared by different routes, the film thicknesses were varied from ~50 nm to ~200 nm by changing the number of spin-coating layer; one layer corresponds to ~50 nm according to scanning electron microscopy (SEM) observation.

Characterization

The crystallographic structure and the texturing degree of thin films were analyzed by X-ray diffraction (XRD, D/max250, Rigaku, Japan) using Cu-Kα radiation (λ=1.5406Å). A field emission scanning electron microscope (FE-SEM, LEO1530, Germany) was used to characterize the surface and cross-section morphologies. The leakage, ferroelectric and dielectric measurements were performed using a ferroelectric tester (Multiferroic, Radiant Technology, USA) and an impedance analyzer (4294A, Agilent, USA). Pt top electrodes (~100 nm in thickness and 400 μm in diameter) were sputter-deposited onto the films through a shadow mask for electrical measurements. Piezoelectric response was characterized by using a piezoresponse force microscope (PFM, MFP-3D, Asylum Research, USA) with a Pt-coated cantilever (Olympus AC240, nominal spring constant 2 N m^{-1}, resonant frequency 70 kHz).

3 Results and Discussion

Microstructure and morphology

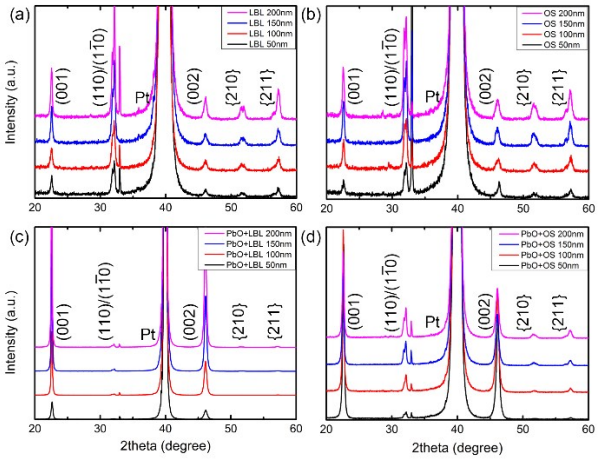

Fig. 1. XRD patterns of $BiFeO_3$ thin films prepared by different routes: (a) LBL, (b) OS, (c) PbO+LBL and (d) PbO+OS.

The XRD patterns of the four groups of samples are shown in Fig. 1(a)-(d). The diffraction peaks are indexed according to the pseudocubic structure. By matching the detected peaks with PDF card of $BiFeO_3$ (PDF#72-2112), no secondary phase was found.[22] It can be inferred from Fig. 1(a) and 1(b) that without PbO seeds the resultant thin films possess a random orientation in which (110) and (1-10) peaks have the highest intensity, as is consistent with PDF card. With increasing thickness, the relative intensities of the peaks of LBL and OS samples are retained though all the peaks become stronger. However, as presented in Fig. 1(c) and 1(d), for the films grown with PbO seeds, (001) and (002) peaks are much higher than others, about four orders of magnitude higher than {210} and {211}, indicating a (001)-textured structure. What's more, with increasing thickness, the (001) peak of PbO+LBL samples is intensified, whose intensity is even comparable to that from Pt bottom electrode. While for PbO+OS samples, {110}, {210} and {210} peaks are much more obvious than PbO+LBL ones and become higher in thicker films, corresponding to a lower texturing degree.

For quantification, the texturing degree was determined by the following equation:

$$\alpha_{001} = \frac{I(001) + I(002)}{\sum I(khl)}$$

where *I*(hkl) is the XRD peak intensity of (hkl) crystal plane and all the observed peaks were taken into account. Since (002) plane is parallel to (001) plane, the numerator includes contributions from both peaks. As for $BiFeO_3$, theoretical value of α_{001} is 29.2% according to PDF card (PDF#72-2112). The degrees of (001) orientation of samples grown by different routes with various thicknesses are depicted in Fig. 2 altogether for comparison. The α_{001} of LBL and OS samples changes little with thickness and is consistent with the theoretical value which is drawn in red dash line. However, α_{001} of $BiFeO_3$ thin films with PbO seeds shows completely contrary thickness-dependent trends when subjected to different annealing processes. For PbO+LBL annealing samples, α_{001} increases slightly with thickness and reaches as high as 98.3% at 200 nm, while for PbO+OS samples, α_{001} decreases as

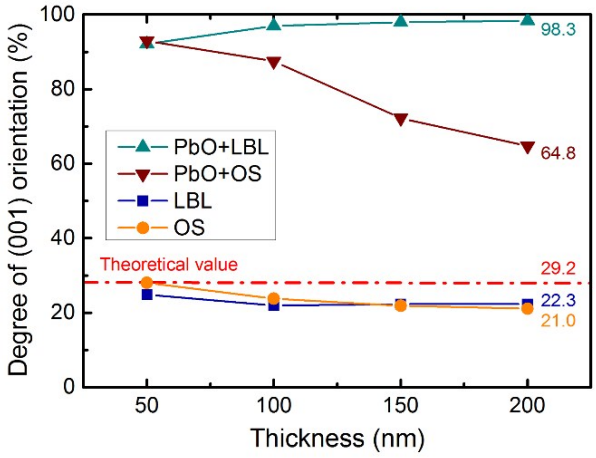

Fig. 2. Thickness dependence of (001) orientation degree of thin films prepared by different routes.

the film gets thicker and drops to 62.8% at 200 nm. The XRD results manifest that PbO seeds are effective in inducing a textured structure and layer-by-layer annealing process is superior to one-step annealing method in maintaining textured structure for thicker films.

Further XRD experiments were conducted on PbO+LBL thin films with high α_{001} values. Step scanning and rocking curves of (002) peak of the samples with various thicknesses are shown in Fig. 3(a) and 3(b), respectively. Peak positions are indexed in Fig. 3(a) to demonstrate the peak shift for various thicknesses. Out-of-plane lattice parameter is calculated based on the peak position of (002) and is drawn in Fig. 3(c) as a function of thickness, together with α_{001} as well as FWHM (full width at half maximum) value which is derived from rocking curve of (002) peak in Fig. 3(b). As thickness increases, FWHM value decreases, again confirming that the degree of texture is higher in thicker films than that in thinner films. Besides, the out-of-plane lattice parameter became larger but is always smaller than the theoretical value 3.96 Å for $BiFeO_3$ bulk materials.[5] This may be associated with stress relaxation: tensile thermal stress is generated during the cooling process due to larger thermal expansion coefficient of $BiFeO_3$ than that of Si.[23,24] The constraint effect resulted in an extension of in-plane lattice parameter and a contraction of out-of-plane lattice parameter. As thickness increases, the thermal stress is gradually released, thus leading to the increment of out-of-plane lattice parameter. In addition, the relatively small lattice parameter of 200-nm-thick sample suggests that the stress is not fully relaxed even at 200 nm thickness, which is thicker than 60 nm in epitaxial $BiFeO_3$ thin films.[25] The larger relaxation thickness can be ascribed to the different origins of stress: for epitaxial thin films, stress originates from lattice mismatch between the films and substrates, which is mainly concentrated at the interface and relaxes quickly, while for the textured films, stress comes from thermal contraction that acts on the whole samples. The same phenomenon was also observed in other textured perovskite thin films.[26]

Fig. 4(a) shows the SEM images of PbO seeds formed on the substrate surface as marked by the red circles. The PbO seeds are distributed on the substrate evenly with an approximately cuboid shape. The typical surface morphology of highly (001)-oriented 200-nm-thick $BiFeO_3$ film processed by PbO+LBL method is presented in Fig. 4(b). The films are dense and crack-free with an average grain size of 50-60 nm. All other samples show similar uniform microstructures and grain sizes regardless of thickness and annealing method. Fig. 4(c)-4(f) show the cross-sectional images of 200 nm thin films prepared in different procedures. According to the calibrated results from SEM images, the accurate thicknesses for these four samples are 233 nm, 224 nm, 197 nm and 196 nm, respectively. For convenience, these four-layer samples are still referred as 200 nm in the following parts. It should be noted that columnar crystals are formed in the PbO+LBL sample, being different from other samples which show clear boundaries of equiaxial grains. The comparison of cross-sectional morphologies implies the crystal growth mechanism of highly textured thin films and how the annealing procedure affects the texture, which will be discussed later.

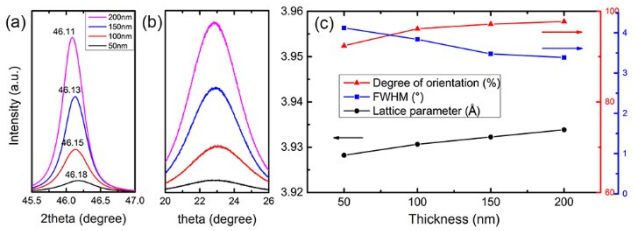

Fig. 3. (a) Step scanning XRD profiles of (002) peaks of PbO+LBL thin films; (b) rocking curves of (002) peaks of PbO+LBL films; (c) Texturing degree, FWHM and lattice parameter of PbO+LBL films with different thicknesses.

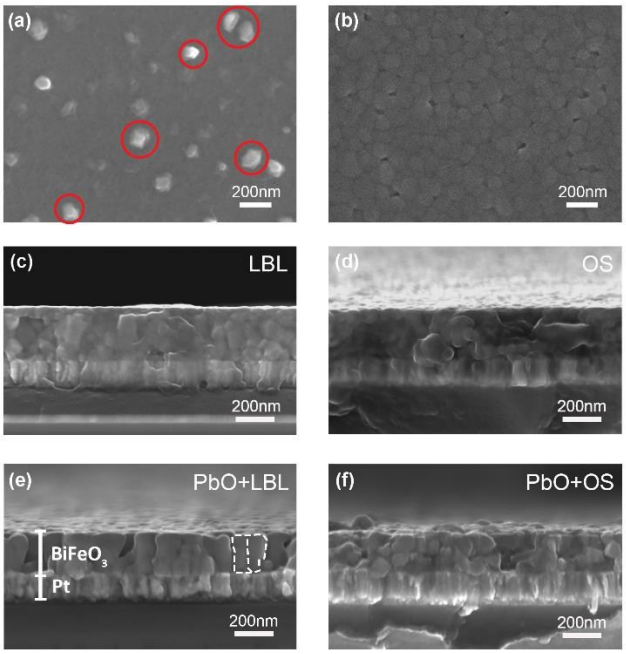

Fig. 4. SEM images of (a) PbO seeds, (b) surface of $BiFeO_3$ thin films, (c) cross-section of 200 nm LBL thin film, (d) cross-section of 200 nm OS thin film, (e) cross-section of 200 nm PbO+LBL thin film and (f) cross-section of 200 nm PbO+OS thin film.

Electrical properties

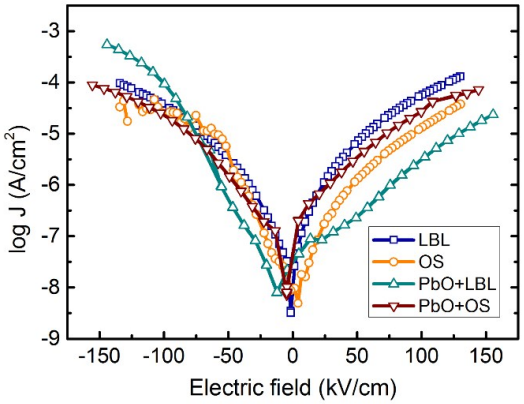

Fig. 5. Leakage of 200-nm-thick samples prepared by different routes.

Electrical tests were conducted on the 200-nm-thick samples prepared by different routes since they exhibited large texturing differences. Fig. 5 shows the leakage current density at room temperature as a function of electric field. At 100 kV cm^{-1}, the current densities of the samples are of the same order of magnitude of 5×10^{-4} A cm^{-2} except for the PbO+LBL one. For PbO+LBL film, when the positive electric field is applied, the current density is ~2×10^{-6} A cm^{-2}, being an order of magnitude lower than that of other samples. This can be ascribed to the formation of columnar crystal structure in which grain boundaries are decreased. It is likely that the reduced current leakage may result from the reduction of grain boundaries in the textured films. However, when the negative electric field is applied, the current density is ~3×10^{-4} A cm^{-2} at 100 kV cm^{-1} in the PbO+LBL thin films, which is slightly higher than other samples The increased leakage in these films is probably due to the interface between $BiFeO_3$ and the bottom electrode, where scattered PbO seeds might weak the contact and create defects, resulting in the accumulation of the electric charges. The asymmetry of leakage current density always emerges due to the difference between top and bottom electrode for the case of epitaxial thin films grown on single crystal substrate. [27]

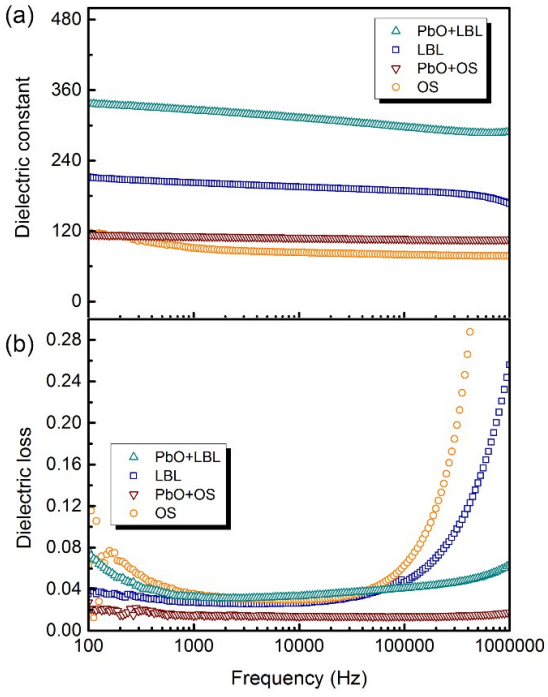

Fig. 6. (a) Dielectric constant and (b) dielectric loss of 200 nm samples grown by different routes.

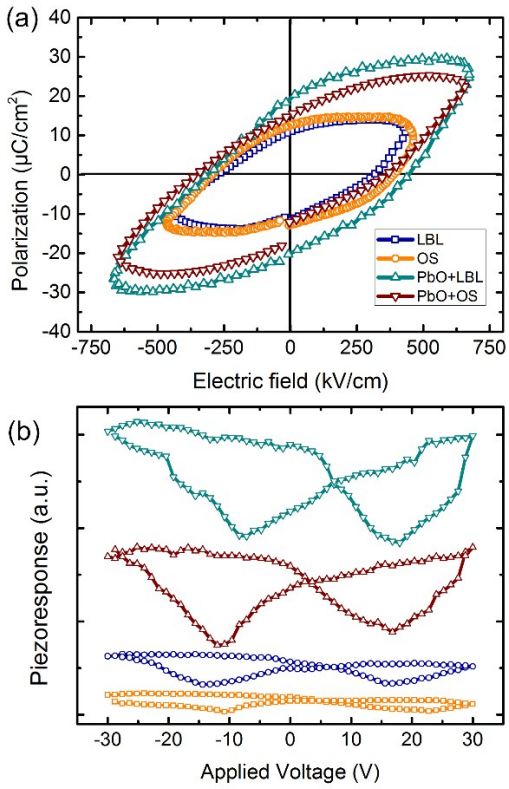

Fig. 7. (a) Ferroelectric and (b) piezoelectric test results of 200-nm-thick samples prepared by different routes.

Fig. 6(a) and 6(b) display the frequency-dependent dielectric constant and corresponding dielectric loss of 200-nm-thick $BiFeO_3$ films prepared by four different routes. The permittivity of all four samples decreases gradually with frequency within the tested range. The permittivity of PbO+LBL samples is as high as 330, comparable to epitaxial $BiFeO_3$ thin films.[28] But, the permittivity of PbO+OS is just about the same value of polycrystalline $BiFeO_3$ thin films or ceramics reported before,[29,30] indicating that the film quality of PbO+LBL sample is better than PbO+OS one. The permittivity of LBL sample also manifests a much higher value than OS one, indicating that layer-by-layer annealing method can improve the dielectric property of the resultant films. Furthermore, dielectric loss rises quickly at 10 kHz for LBL and OS films, implying that some other factors contribute to dielectric constant in these non-textured samples at low frequencies, *i.e.* space charges, which accumulate at crystal boundaries.[23] The space charges may also be the reason for the higher dielectric constant of LBL sample than that of PbO+OS. As for OS samples, though the space charges contributed to dielectric constant, some defects like pores were left inside due to the one-step annealing, which might further decrease the dielectric constant. For the PbO-seeded textured films, dielectric loss values

are quite small and remain at a low level at high frequencies, as can be ascribed to the textured structure which is effective in reducing grain boundaries and space charges, thus improving the film quality.

Ferroelectric test was conducted at 10 kHz and depicted in Fig. 7(a). From the ferroelectric results, it can be seen that (001)-textured $BiFeO_3$ thin films manifest enhanced P_r (~20 μC cm^{-2}) than the non-textured samples. The higher P_r values of PbO+LBL film than PbO+OS film can be ascribed to the improved quality of textured sample. However, the thin films without PbO seeds cannot bare high electric field before breaking down. Though the leakage current of LBL and OS samples are of the same order of PbO+LBL and PbO+OS at 100 kV cm^{-1}, the ferroelectric results illustrate that leakages of non-textured films rises quickly at high electric fields, which leads to the breakdown. Besides, the lower P_r values of these thin films than the theoretical value (P_r ~ 100 μC cm^{-2}) may be due to large leakage of sol-gel-processed $BiFeO_3$ films, especially at a small thickness,[14,15,31] although higher P_r was reported in epitaxially grown $BiFeO_3$ thin films by other methods.[5] For this reason, leakage plays an important role and prevents the imposition of higher voltages. It should be mentioned that the PbO+LBL and PbO+OS samples also showed some leakage features, which may be ascribed to the high leakage feature of $BiFeO_3$.[31] Fig. 7(b) displays the piezoelectric test results, which reveal that all the films manifest the typical "butterfly loop".[32] Signals were acquired from OFF sates, so the electrostatic force was minimized.[33] Similar to ferroelectric results, the PbO-seeded textured films demonstrate large piezoelectric responses and PbO+LBL samples show even higher responses than that of PbO+OS one. The remarkable enhancement can be interpreted by the appearance of columnar crystal structure of PbO+LBL film in which dipoles are sufficiently poled along the electric field, while for PbO+OS samples, more crystal boundaries may not favour the piezoelectric deformation. The comparison indicates that the textured structure has a fairly positive effect for piezoelectric property enhancement if compared with the randomly oriented polycrystalline thin films.

Discussion of texturing origin

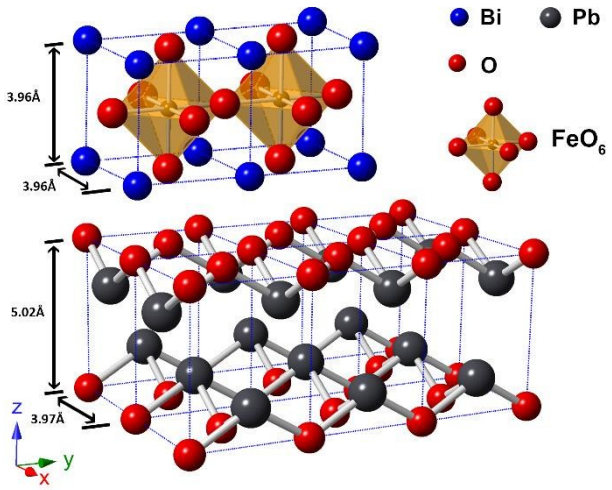

Fig. 8. Crystal structures of $BiFeO_3$ and PbO crystals with (001) orientation.

Fig. 8 displays the schematic crystal structures of $BiFeO_3$ and PbO with (001) orientation. The octahedral tilting of $BiFeO_3$ is neglected and only two pseudocubic lattices are drawn in the figure since the emphasis is laid on lattice parameters. PbO possesses a litharge structure, which is tetragonal with a large *c/a* ratio. After crystallization, the (001) surface of PbO seeds will be on the top side so that surface energy is minimized.[18] Meanwhile, the lattice parameter of $BiFeO_3$ is close to PbO along the in-plane direction. As a result, $BiFeO_3$ is more likely to nucleate on the surface of PbO seeds and inherit the orientation of PbO. Besides, the in-plane lattice parameter of PbO, 3.97 Å, is a little bit larger than that of $BiFeO_3$, which also plays an important role of the tensile stress generated in thin films.[34] Without PbO seeds, $BiFeO_3$ would crystalize from the amorphous state and nucleate randomly on the substrate since Pt(111) plane shows low matching degree with any $BiFeO_3$ crystal planes.

The annealing effect and thickness effect are related with this texturing mechanism. In one-step annealing mode, during the repeated pyrolysis procedures, more defects might be formed and acted as nucleating sites in crystallization stage. The $BiFeO_3$ grains nucleated inside the films tended to be randomly oriented, thus disrupting the existing (001)-textured structure induced by PbO seeds. The thicker the film is, the more defects there are in amorphous $BiFeO_3$. Therefore, α_{001} of PbO+OS samples decreased with thickness and the cross-sectional image manifested the feature of non-textured structure, as is illustrated in Fig. 4(f). While for the case of layer-by-layer annealing mode, since each layer is thin enough, the newly grown grains still showed (001) faces on the surface of sample and served as new nucleation sites without lattice mismatch in the followed deposition procedures. The next layer would crystalize on the existing crystals and retain the orientation. As a result, a highly textured structure was formed with a feature of columnar crystals as shown in Fig. 4(e).

4 Conclusions

In summary, perovskite $BiFeO_3$ thin films with thicknesses from ~50 nm to ~200 nm were prepared on PbO-seeded Pt(111)/Ti/SiO_2/Si substrates by the sol-gel method adopting layer-by-layer annealing and one-step annealing routes. PbO seeds can lead to highly (001)-textured structure due to the high c/a ratio and similar in-plane lattice parameter to $BiFeO_3$. The degree of (001) orientation was intensified with thickness for the PbO-seeded samples prepared by the layer-by-layer annealing process and reached 98.3% in a 200-nm-thick film. Columnar grains were observed in the highly textured sample, indicating that layer-by-layer annealing method favours the formation of textured structure compared with one-step annealing method. Textured $BiFeO_3$ films showed reduced leakage and enhanced dielectric, ferroelectric and piezoelectric properties. The high quality $BiFeO_3$ thin films integrated on Si substrate would facilitate the application of $BiFeO_3$ in ferroelectric and electromechanical devices.

Acknowledgements

This work was supported by National Nature Science Foundation of China (Grants no. 51332002, 51221291) the Ministry of Science and Technology of China under the Grant 2015CB654605.

Notes and references

1 D. L. Polla and L. F. Francis, *Annu. Rev. Mater. Sci.*, 1998, **28**, 563-597.
2 G. H. Haertling, *J. Am. Ceram. Soc.*, 1999, **82**, 797-818.
3 N. Setter, D. Damjanovic, L. Eng, G. Fox, S. Gevorgian, S. Hong, A. Kingon, H. Kohlstedt, N. Y. Park, G. B. Stephenson, I. Stolitchnov, A. K. Taganstev, D. V. Taylor, T. Yamada and S. Streiffer, *J. Appl. Phys.*, 2006, **100**, 051606.
4 J. Wang, J. B. Neaton, H. Zheng, V. Nagarajan, S. B. Ogale, B. Liu, D. Viehland, V. Vaithyanathan, D. G. Schlom, U. V. Waghmare, N. A. Spaldin, K. M. Rabe, M. Wuttig and R. Ramesh, *Science*, 2003, **299**, 1719-1722.
5 G. Catalan and J. F. Scott, *Adv. Mater.*, 2009, **21**, 2463-2485.
6 D. Sando, A. Barthelemy and M. Bibes, *J. Phys. Condens. Matter*, 2014, **26**, 473201.
7 X. Tang, L. Hu, J. Yang, L. Chen, J. Dai, W. Song, Z. Yang, X. Zhu and Y. Sun, *RSC Adv.*, 2014, **4**, 32738-32743.
8 B. Li, C. Wang, G. Dou and Z. Wang, *RSC Adv.*, 2014, **4**, 55889-55896.
9 S. H. Baek, C. M. Folkman, J. W. Park, S. Lee, C. W. Bark, T. Tybell and C. B. Eom, *Adv. Mater.*, 2011, **23**, 1621-1625.
10 R. J. Zeches, M. D. Rossell, J. X. Zhang, A. J. Hatt, Q. He, C. H. Yang, A. Kumar, C. H. Wang, A. Melville, C. Adamo, G. Sheng, Y. H. Chu, J. F. Ihlefeld, R. Erni, C. Ederer, V. Gopalan, L. Q. Chen, D. G. Schlom, N. A. Spaldin, L. W. Martin and R. Ramesh, *Science*, 2009, **326**, 977-980.
11 S. H. Baek, J. Park, D. M. Kim, V. A. Aksyuk, R. R. Das, S. D. Bu, D. A. Felker, J. Lettieri, V. Vaithyanathan, S. S. Bharadwaja, N. Bassiri-Gharb, Y. B. Chen, H. P. Sun, C. M. Folkman, H. W. Jang, D. J. Kreft, S. K. Streiffer, R. Ramesh, X. Q. Pan, S. Trolier-McKinstry, D. G. Schlom, M. S. Rzchowski, R. H. Blick and C. B. Eom, *Science*, 2011, **334**, 958-961.
12 G. Panomsuwan, O. Takai, N. Saito and G. L. Brennecka, *J. Am. Ceram. Soc.*, 2014, **97**, 1383-1385.
13 C. Ruangchalermwong, J.-F. Li, Z.-X. Zhu and S. Muensit, *J. Phys. D: Appl. Phys.*, 2008, **41**, 225302.
14 C.-C. Leu, T.-J. Lin, S.-Y. Chen, C.-T. Hu and P. Paranthaman, *J. Am. Ceram. Soc.*, 2015, **98**, 724-731.
15 H. W. Chang, F. T. Yuan, S. H. Tien, K. T. Tu, C. R. Wang and S. U. Jen, *J. Appl. Phys.*, 2014, **115**, 17D912.
16 K. Kariya, T. Yoshimura, S. Murakami and N. Fujimura, *J. J. Appl. Phys.*, 2014, **53**, 09PA14.
17 W. Gong, J.-F. Li, X. Chu, Z. Gui and L. Li, *J. Appl. Phys.*, 2004, **96**, 590.
18 W. Gong, J.-F. Li, X. Chu, Z. Gui and L. Li, *Acta Mater.*, 2004, **52**, 2787-2793.
19 C. Zhong, X. Wang, Y. Wu and L. Li, *J. Am. Ceram. Soc.*, 2010, **93**, 3993-3996.
20 C. Zhong, X. Wang, L. Guo and L. Li, *Thin Solid Films,* 2015, **580**, 52-55.
21 Z. Xie, Z. Yue, B. Peng, J. Zhang, C. Zhao, X. Zhang, G. Ruehl and L. Li, *Appl. Phys. Lett.*, 2015, **106**, 202901.
22 Y. Wang and C.-W. Nan, *J. Appl. Phys.* , 2008, **103**, 024103.
23 W. Sun, J.-F. Li, Q. Yu and L.-Q. Cheng, *J. Mater. Chem. C,* 2015, **3**, 2115-2122.
24 W. Sun, J.-F. Li, F. Zhu, Q. Yu, L. Q. Cheng and Z. Zhou, *Phys. Chem. Chem. Phys.*, 2015, **17**, 19759-19765.
25 H. Ma, L. Chen, J. Wang, J. Ma and F. Boey, *Appl. Phys. Lett.*, 2008, **92**, 182902.
26 J.-F. Li, Z.-X. Zhu and F.-P. Lai, *J. Phys. Chem. C,* 2010, **114**, 17796-17801.
27 T. L. Qu, Y. G. Zhao, D. Xie, J. P. Shi, Q. P. Chen and T. L. Ren, *Appl. Phys. Lett.*, 2011, **98**, 173507.
28 S. H. Lim, M. Murakami, J. H. Yang, S. Y. Young, J. Hattrick-Simpers, M. Wuttig, L. G. Salamanca-Riba and I. Takeuchi, *Appl. Phys. Lett.*, 2008, **92**, 012918.
29 S.-Z. Lu, X. Qi and P. Joy, *J. Am. Ceram. Soc.*, 2014, **97**, 2185-2194.
30 X. Tang, J. Dai, X. Zhu, J. Lin, Q. Chang, D. Wu, W. Song, Y. Sun and X. Tan, *J. Am. Ceram. Soc.*, 2012, **95**, 538-544.
31 J. Zeng, Z. H. Tang, M. H. Tang, D. L. Xu, Y. G. Xiao, B. W. Zeng, L. Q. Li and Y. C. Zhou, *J. Sol-Gel Sci. Technol.*, 2014, **72**, 587-592.
32 S. Jesse, A. P. Baddorf and S. V. Kalinin, *Appl. Phys. Lett.*, 2006, **88**, 062908.
33 J. Li, J.-F. Li, Q. Yu, Q. N. Chen and S. Xie, *Journal of Materiomics*, 2015, **1**, 3-21.
34 D. J. Payne, R. G. Egdell, D. S. L. Law, P.-A. Glans, T. Learmonth, K. E. Smith, J. Guo, A. Walsh and G. W. Watson, *J. Mater. Chem.*, 2007, **17**, 267.

Graphical Abstract

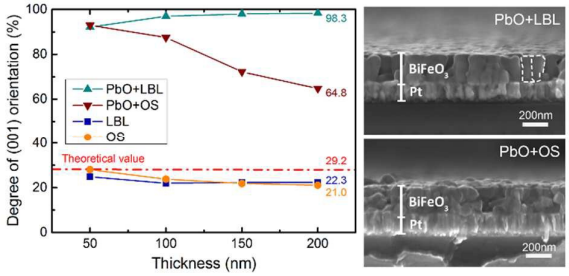

Highly (001)-oriented $BiFeO_3$ thin films were grown on Pt(111)/Ti/SiO_2/Si substrates with PbO seeding nanocrystals by a layer-by-layer annealing method